International Journal of Pharmaceutics 417 (2011) 17–31

Contents lists available at ScienceDirect

International Journal of Pharmaceutics

journal homepage: www.elsevier.com/locate/ijpharm

The contribution of Raman spectroscopy to the analysis of phase transformations in pharmaceutical compounds

Alain Hédoux[a,b,c,*], Yannick Guinet[a,b,c], Marc Descamps[a,b,c]

[a] University Lille Nord de France, F-59000 Lille, France
[b] USTL, UMET, F-59650 Villeneuve d'Ascq, France
[c] CNRS, UMR 8207, F-59650 Villeneuve d'Ascq, France

ARTICLE INFO

Article history:
Received 26 October 2010
Received in revised form 5 January 2011
Accepted 17 January 2011
Available online 21 January 2011

Keywords:
Raman spectroscopy
Phonon Raman spectrum
Vibrational density of states
Polymorphic transformations
Indomethacin
Caffeine

ABSTRACT

We show in this paper the contribution of the whole Raman spectrum including the phonon spectrum, to detect, identify and characterize polymorphic forms of molecular compounds, and study their stability and transformation. Obtaining these kinds of information is important in the area of pharmaceutical compounds. Two different polymorphic systems are analyzed through investigations in indomethacin and caffeine exposed to variable environmental conditions and various stresses, as possibly throughout the production cycle of the active pharmaceutical ingredient. It is shown the capability of the low-frequency Raman spectroscopy to reveal disorder in the crystalline state, to detect small amorphous or crystalline material, and to elucidate ambiguous polymorphic or polyamorphic situations.

1. Introduction

Organic molecular compounds are characterized by a pronounced contrast between strong covalent intramolecular interactions and soft van der Waals intermolecular attractions or hydrogen bonding association. Intermolecular interactions are responsible for specific physical properties of molecular compounds (rich polymorphism, low melting temperature, ...),while covalent bonds maintain the cohesion within the molecule despite of atom–atom intermolecular interactions. In the framework of the rigid body model, molecular motions in organic solids can be classified in three categories. (i) The internal motions, corresponding to vibration within the molecule, (ii) the semi-internal (or external) motions corresponding to very low-frequency rotations of a group of atoms within the molecule or the whole of the molecule, and (iii) the external motions associated to intermolecular and collective vibrations, named lattice vibrations or phonons in the crystalline state, and consisting in a vibrational density of states in the solid amorphous state. Raman spectroscopy gives the original opportunity to analyze these different kinds of motions. External vibrations play an important role in determining properties of molecular aggregates, providing at molecular levels information on the stability of the physical state, and the nature of solid state transformations. Raman spectroscopy gives direct information on phase transformation mechanisms, from in situ investigations on molecular compounds exposed to a wide variety of environmental stresses, since no special sample preparation is required. Consequently, Raman spectroscopy has important applications in the field of pharmaceutical sciences (Chieng et al., 2009; Kogermann et al., 2007; Okumura and Otsuka, 2005; Strachan et al., 2004; Taylor and Zografi, 1998; Vankeirsbilck et al., 2002), especially in the area described below.

The development of pharmaceutical solid formulations requires important information on the characteristics and the physical nature of solid phases including crystalline and amorphous solids. Molecular compounds go through several stages of processing (milling, freeze-drying, spray-drying, pressurizing) for packaging as solid-dosage form. During their storage, drugs may be exposed to a wide range of temperatures and humidities which can lead to different kinds of phase transformations (crystallization from an amorphous state or crystal–crystal transitions). The stability conditions of the polymorphs and the amorphous state have to be determined, and polymorph selection and control is crucial.

Tabletting involves the direct compression of the active pharmaceutical ingredient (API) in the 40–400 MPa pressure range. In some cases, the application of such a pressurization makes possible the transformation of a metastable form toward the stable

* Corresponding author. Tel.: +33 320434677; fax: +33 320436857.
E-mail address: alain.hedoux@univ-lille1.fr (A. Hédoux).

0378-5173/$ – see front matter © 2011 Elsevier B.V. All rights reserved.
doi:10.1016/j.ijpharm.2011.01.031

crystalline form, as observed for caffeine (Chan and Doelker, 1985). In the general context of the understanding the possible pressure-induced transformations of APIs under grinding or tabletting, the high-pressure studies of pharmaceuticals using diamond-anvil cells (DAC) is growing in importance (Boldyreva, 2007; Boldyreva et al., 2002, 2006; Fabiani et al., 2003, 2007; Fabiani and Pulham, 2006).

It is well known that bio-availability is enhanced in the amorphous state of the drug, and can be drastically different in crystalline forms, with implications for administration of correct dosage for the patient. In the case of crystalline drugs exhibiting very poor water solubility, their conversion into amorphous state offers a strategy for improving dissolution rates and hence bioavailability (Yamamoto et al., 1970). Indomethacin is typically a poorly water-soluble drug (Matsumoto and Zografi, 1999), which is known to exhibit different crystallization processes, even well below the glass transition temperature (Hédoux et al., 2009; Yoshioka et al., 1994) (T_g), depending on how the amorphous state is prepared (Otsuka and Kaneniwa, 1988; Wu and Yu, 2006a; Yoshioka et al., 1994). Polymers such as polyvinylpyrrolidone (PVP), are used to enhance the physical stability of amorphous drugs. It is thus important to understand at the molecular level the mechanisms by which polymers or small molecules stabilize amorphous drug. Understanding how do excipient solid dispersions control better the stability of the API is crucial to predict its conversion toward the crystalline state.

Grinding is often used as an alternative to reach the amorphous state without chemical degradation induced by heating or dissolution (Bahl and Bogner, 2006; Shakhtshneider et al., 2007; Willart and Descamps, 2008). However the material can experience localized compression, shear stress and possible localized heating. The amorphous ground powder can be characterized by physical properties (Gibbs energy), different from those of the glass obtained by quenching the liquid state, and leading to distinctive chemical and thermal stability of the amorphous powder. It is crucial to understand the mechanism of amorphization in order to predict the physical properties of the amorphous ground powder.

In the most of molecular drugs, molecular associations through hydrogen-bonding are generally distinctive of the different forms in the (P,T) phase diagram, and phase transitions are closely related to the stability of the H-bond network.

The most common methods applied for solid state analysis are X-ray powder diffraction, differential scanning calorimetry and different spectroscopic techniques. Raman Spectroscopy is fast, non-destructive and probe structural changes at different levels: molecular conformation (Hedoux et al., 2006), short-range order (local molecular environment (Denicourt et al., 2003), molecular associations through hydrogen bonding (Wypych et al., 2007)) and long-range order (Denicourt et al., 2003), and can be used to discriminate the earlier stages of crystallization from structural changes in the local order of amorphous states (Hedoux et al., 1998; Hédoux et al., 2000; Wypych et al., 2007). The Raman spectroscopy has a major role in analysis and material characterization within the pharmaceutical industry. It is widely used as a quality-control assurance tool, for chemical identification, or analyzing quantitatively drug substances in the context of their solid-state form, mainly from measurements performed in the 300–1800 cm^{-1} region considered as molecular structure fingerprints of an analyte. In this paper we report detailed Raman investigations in two different polymorphic systems (indomethacin and caffeine), to show the contribution of the low-frequency spectrum in the description of phase transformations or mixed coexisting phases. It is also shown that Raman spectroscopy can be used as an indirect structural probe for understanding of the mechanism of phase transformations, and for the determination of the parameters responsible for the stability of the physical states.

2. Materials and methods

2.1. Materials

The γ form of indomethacin (γ-IMC) with a purity of 99% is supplied from FLUKA and used as received. **The α form of indomethacin** was prepared by dissolution in ethanol at 80 °C and precipitation with water at room temperature as described by Kaneniwa et al. (1985). The amorphous state was obtained by two different routes: the quench of the melt from 443 K down to 295 K ($T_g - 20$ K) at 5 K/min, producing a thermal glass (QL), and the grinding at 77 K leading to a ground amorphous solid (GAS). It was previously shown that **grinding** below the glass transition temperature has a high potentiality to convert the crystal into the amorphous solid state (Descamps et al., 2006). Moreover it was previously found, from X-ray investigations (Otsuka and Kaneniwa, 1988; Otsuka et al., 1986), that grinding of γ IMC just below T_g led to partially amorphous material whereas low temperature grinding led to amorphous powder. Consequently cryogenic grinding method is used to obtain amorphous IMC powder.

Caffeine (98.5% purity) was purchased from Acros Organics and was purified by cold sublimation: caffeine was sublimated at 220 °C and 10^{-3} torr onto a cold finger (at 12 °C). Using this method, pure phase I is directly obtained in a metastable state. The domain of stability of phase I is lying between the II → I transition temperature (T_t = 153 °C) and the melting temperature (T_m = 236 °C). Pure phase II is obtained by maintaining purified caffeine in an oven at 90 °C during several months.

2.2. Raman spectroscopy

2.2.1. Basic theory

The requirement for spontaneous Raman activity is a change in the electronic polarizability of the analyzed molecule. The monochromatic light from a laser is generally used to irradiate the sample. A photon interacts with the electron cloud and the bonds of the molecule. In classical terms, the interaction can be viewed as a perturbation of the molecule's electric field. When a molecule is exposed to an electric field, electrons and nuclei are forced to move in opposite directions. A dipole moment is induced which is proportional to the electric field strength and to the molecular polarizability α. A molecular vibration described by the normal coordinate $q_i = q_i^0 \cos(2\pi\nu_i t)$ can be observed in the Raman spectrum if the condition

$$\left(\frac{\partial\alpha}{\partial q}\right)_0 \neq 0 \quad (1)$$

is satisfied. In quantum mechanics, a photon excites the molecule from the ground state to a virtual energy state. When the molecule relaxes it emits a photon and returns to an energy state different from the original state. The difference energy between the original and final states leads to a frequency shift ($\Delta\nu$) between the emitted photon's frequency (ν_i) and that of the excitation wavelength (ν_0), the so-called Raman shift. If the final state is more energetic than the initial state, the Raman shift ($\Delta\nu = \nu_0 - \nu_i$) is designated as a Stokes shift. In the opposite case, the energy transfer corresponds to $\Delta\nu = \nu_0 + \nu_i$, called anti-Stokes shift. Most of the light is elastically scattered in different directions (Rayleigh scattering). The inelastically back scattered light corresponding to Stokes shift is usually analyzed, since it is characterized by an intensity higher than that corresponding to the anti-stokes spectrum. This characteristic can be explained from the consideration that the Stokes transition is much more probable than the anti-stokes transition.

The ratio of Stokes to anti-Stokes intensities is given by (Long, 1977)

$$\frac{(\nu_o - \nu_i)^4}{(\nu_o - \nu_i)^4} \exp\left(\frac{h\nu_i}{kT}\right) \quad (2)$$

This equation can be used for the determination of intrinsic sample temperature, by fitting simultaneously the Stokes and anti-Stokes intensities. The intensity of the Stokes Raman spectrum is mainly proportional to (Long, 1977):

$$I_{Raman} \propto NI_0\,[n(\nu)+1](\nu_0 - \nu_i)^4 \left[\vec{e}_f \left(\frac{\partial\overline{\overline{\alpha}}}{\partial q_i}\right)\vec{e}_j\right]^2 \quad (3)$$

where N is the number of molecules $-n(\nu) = [1 - \exp(h\nu/kT)]^{-1}$, the bose factor – $\overline{\overline{\alpha}}$, the polarizability tensor corresponding to the (q_i, ν_i) vibration – and $\vec{e}_j$, $\vec{e}_f$ correspond to the unit vectors of the incident and scattered electric field. It is worth noting that the bose factor has a great influence on the low-frequency Raman line shape ($\nu < 200\,cm^{-1}$).

2.2.2. Experimental procedures

Two kinds of spectrometers can be used for collecting Raman spectra, the Fourier transform (FT-Raman) or dispersive Raman spectrometers. They are composed of four main components: (i) the laser source of monochromatic radiation, (ii) a sample illumination system and light connection optics, (iii) a device for the analysis of the scattered light (spectrometer), (iv) and a sensitive detector such as a charge-coupled device (CCD). The difference between both types of spectrometer bases essentially on the device (iii): a grating dispersing system for dispersive Raman spectrometers, or an interferometer for FT-Raman spectrometers. Most of FT-Raman spectrometers use a Nd:YAG laser (1.064 μm) with a near-infrared interferometer coupled to either a liquid nitrogen cooled germanium or indium gallium arsenide detector. The main advantages are (i) the reduction in the number of samples that exhibit laser-induced fluorescence, (ii) the ease of operation as with an FT-IR spectrometer, (iii) and the high spectral resolution with good wavelength accuracy. However, the use of FT-Raman spectrometers present the disadvantage of being relatively unsuitable for sample environment (temperature, pressure, humidity, ...). Dispersive Raman spectrometers use multi-channel (CCD) detectors, with extremely low intrinsic noise and a high quantum efficiency. The benefits for dispersive Raman are far higher sensitivities and far lower detection limits than FT-Raman. The shorter wavelengths of lasers associated with dispersive Raman increase the sensitivity of the spectrometer, because of the ν^4 scattering efficiency dependency. As a consequence, the data acquisition times are much shorter than for FT-Raman methods, that is important for the study of fast transformation kinetics. The spectra presented in this paper have been obtained from dispersive Raman spectrometers. The performances of these last ones result from the adequacy between a good resolution and rejection of the laser line, and a sufficient intensity, imposed by the dispersion system. Modern instrumentation almost universally employs notch or edge filters for laser rejection, and spectrograph (monochromator). However, in this case the analysis of the low-frequency range (<150 cm^{-1}) is prohibited. The use of multiple dispersion stages (double and triple monochromators) mounted with a long focal length allow the detection of Raman-active modes with frequencies as low as 2–5 cm^{-1}.

Depending on the nature of the analysis, the important volumes or heterogeneities or microscopic samples, we shall distinguish two types of installation; the conventional installation or the macroanalysis, and the installation micro Raman suitable for micro analyses. Raman investigations under pressure are typically performed on microscopic samples located in DACs, and then micro-Raman installation is systematically used for pressure analyzes. For micro Raman, the sample holder is a XYZ table equipped with a microscope composed of high numerical aperture objectives. This type of equipment allows the quantitative analyzes of mixtures (Strachan et al., 2004) or mapping of solid dispersions (Breitenbach et al., 1999).

Raman spectra presented in this paper have been mainly obtained on a XY Dilor spectrometer. It is characterized by a double monochromator grating dispersing system, composed of four mirrors with a long focal length (800 mm), coupled to an additional grating system corresponding to the spectrograph. Obtaining an optimal rejected light requires the well-adapted positioning of the monochromator with regard to the spectrometer, and allows the analysis of the low-frequency domain down to 2 cm^{-1}. The back-scattering Raman spectra were recorded using the 514.5 nm line of a mixed Argon–Krypton Coherent laser. The entrance and exit slits are opened to 150 μm, determining for the incident radiation a resolution nearly less than 1.5 cm^{-1} in the low-frequency range. For high-pressure investigations, the laser beam focused using a long-working distance objective (×50) of an Olympus microscope.

Raman mapping was performed using Renishaw's inVia Raman microscope, comprising a single-grating spectrograph coupled to an optical microscope. Using the 514.5 nm laser line leads to a spectral resolution of about 2.5 cm^{-1} in the fingerprint region. Raman images were obtained using the "StreamLine Plus" technology. StreamLine Plus uses optics within the inVia Raman microscope to illuminate a line on the sample. Data are swept synchronously across the detector as the line moves across the sample, and are read out continuously. The spatial resolution is mainly determined by the choice of microscope objective, wavelength of laser line, and settings of detection.

2.2.3. Analysis of Raman spectra of molecular materials

In molecular drugs and more generally in organic molecular materials, the intramolecular bonding is very strong compared with the weak intermolecular bonding. Consequently there is a disparity between force constants in molecular solids which is reflected in the Raman spectra by a spectral gap between external and internal bands, which is dependent on the molecule. In this context, it can be considered as a general property of the molecular compounds that the internal modes segregate from the low-frequency vibrations.

For a crystalline state characterized by N molecules in the unit cell corresponding to $6N$ possible motions, the number of Raman active-modes is mainly dependent on the crystalline symmetry and can be determined from group theoretical analysis. The number of internal Raman active modes results from the considerations of the molecular and the crystalline symmetries, reflecting the local molecular arrangement. Consequently, Raman spectroscopy can be considered as an indirect structural probe, providing information about the long-range order and the local molecular environment from the respective analyzes of the low-frequency Raman spectrum (LFRS) and the spectrum of internal modes in the crystal.

The amorphous solid state can be roughly distinguished from the crystalline state by the loss of periodicity. The main consequences are the absence of phonon peaks in the LFRS and the inhomogeneous broadening of internal modes related to a distribution of molecular environments. It was demonstrated that the intensity of the Stokes LFRS can be related to the vibrational density of states (VDOS) from (Galeener and Sen, 1978; Shuker and Gammon, 1970):

$$I_{Raman}(\nu) = \frac{[n(\nu)+1]}{\nu} C(\nu)G(\nu) \quad (4)$$

In the Eq. (4), $G(\nu)$ reflects the collective vibrations, and has usually a very broad band shape corresponding to the rough envelope of the phonon peaks in the underlying crystalline state. $C(\nu)$ is the light-vibration coupling coefficient.

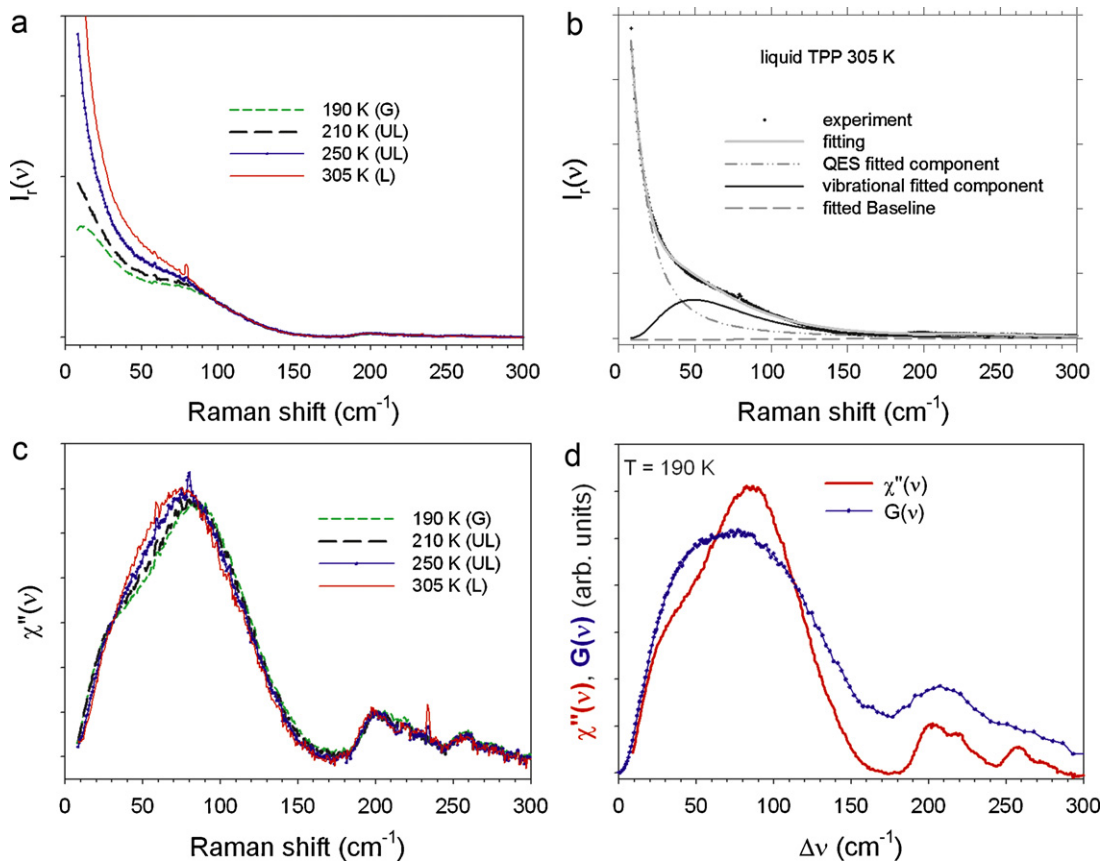

Fig. 1. Representations of the low-frequency spectrum of TPP. (a) Temperature dependence of the reduced intensity in the glassy (G), undercooled liquid (UL) and liquid (L) states. (b) Description of the fitting procedure of the reduced intensity in the liquid state of TPP. (c) Temperature dependence of the Raman susceptibility in the glassy, undercooled liquid and liquid states of TPP. (d) Comparison between the Raman susceptibility and the VDOS determined from inelastic neutron scattering experiments, in the glassy state of TPP.

In addition to $G(\nu)$, the LFRS exhibits a specific low-frequency excitation to the glassy state named the Boson Peak (BP), recognized to be connected to the excess of VDOS and considered as the universal vibrational signature of the glassy state (Achibat et al., 1993; Duval et al., 1990). This low-frequency peak can be detected by inelastic neutron scattering and by low-frequency Raman spectroscopy. In fragile systems in the Angell classification (Angell, 1991), and more generally in organic molecular compounds, the BP overlaps with the low-frequency contribution of $G(\nu)$ and thus is hardly detectable in this type of materials, contrarily to strong systems like oxide glasses (Pelous et al., 1995). Upon heating the glassy state, another type of excitations develops, named the quasi-elastic scattering (QES). The QES corresponds to large amplitude motions of the molecule or a group of atoms in the molecule, and is strongly dependent on the temperature, in opposition to the collective motions of the VDOS which have generally a quasi-harmonic behavior. This component is lying over the 0–100 cm^{-1} range, and thus overlaps with the contribution of collective vibrations. Raman spectroscopy gives the opportunity to analyze both kinds of motions.

In disordered systems, the LFRS is usually converted into the reduced Raman spectrum according to

$$I_r(\nu) = I_{Raman}\frac{(\nu)}{([n(\nu)+1]\nu)} \quad (5)$$

Reduced intensity is then free of line shape distortion due to thermal population effects. In this representation, the spectrum is dominated by the QES intensity in the very low-frequency range (<100 cm^{-1}), which strongly increases upon heating above T_g. The reduced intensity is plotted in Fig. 1a, for a molecular compound (triphenyl phosphite, TPP) in the glassy state (190 K), the undercooled liquid (213 and 253 K) and liquid (305 K) states. Fig. 1a confirms that the QES is the predominant contribution in the reduced spectrum, and is clearly temperature dependent. The analysis of the low-frequency vibrations requires the separation of the monomolecular (QES) and collective motions. A fitting procedure is used to determine the QES which is described by a lorentzian lineshape centred at $\Delta\nu = 0$, while collective vibrations are represented by a log–normal distribution (Malinovski et al., 1991). The result of the fitting procedure is plotted in Fig. 1b. The QES is subtracted from the reduced intensity to analyze the collective vibrations, and the reduced intensity is then transformed into the Raman susceptibility according to

$$\chi''(\nu) = I_r(\nu).\nu = \frac{C(\nu)}{\nu}G(\nu) \quad (6)$$

Equation (6) clearly shows that the Raman intensity is not rigorously proportional to the VDOS, since the $C(\nu)$ coupling coefficient is dependent on ν. However, $C(\nu)$ has usually a linear frequency dependence in the region of the BP (Achibat et al., 1993; Hedoux et al., 2001a; Novikov and Duval, 1994). Consequently the Raman susceptibility can be considered as representative of the VDOS. The Raman susceptibility is plotted in Fig. 1c at different temperatures in the glassy and undercooled liquid states. In Fig. 1d, the Raman susceptibility in the glassy state of TPP is compared at 190 K, to the VDOS obtained from inelastic neutron scattering experiments (Hedoux et al., 2001a) performed on IN6 spectrometer at the Institute Laue Langevin (ILL, Grenoble). This figure confirms that the Raman susceptibility is slightly different from the VDOS, but it is clearly observed that Raman spectroscopy provides better resolved

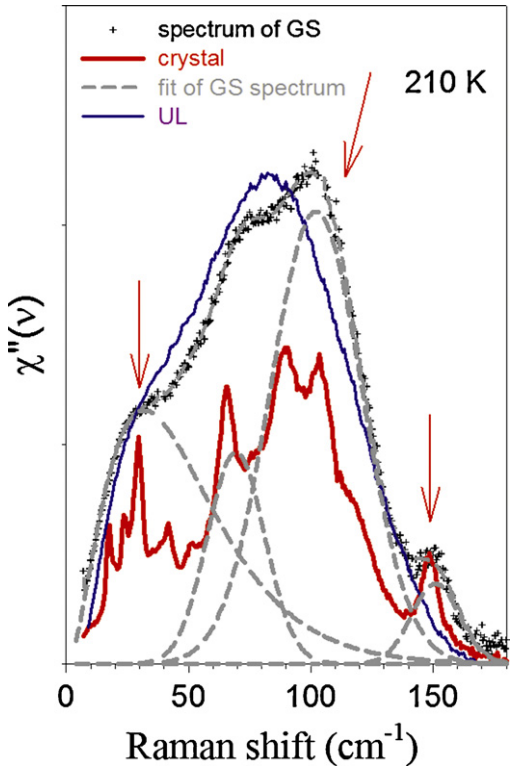

Fig. 2. $\chi''(\nu)$-spectra of the undercooled liquid state (UL), the metastable glacial state (GS) and the stable crystal of TPP at the same temperature. The bands plotted in dashed lines correspond to the fitting procedure of the Raman susceptibility of the glacial TPP. The arrows localize the main spectral changes between the undercooled liquid and the glacial states.

spectra than inelastic neutron scattering. TPP has been widely investigated, because it was suspected to undergo a polyamorphic transition under atmospheric conditions (Ha et al., 1996; Senker and Rossler, 2001; Tanaka et al., 2004), above T_g (~202 K). Indeed a first order phase transition was detected between the undercooled liquid and an apparently amorphous state named the glacial state (GS). Only low-frequency Raman investigations (Hedoux et al., 1998, 2001a,b; Hédoux et al., 2000, 2006) give the clear evidence that the GS was not really amorphous, and was composed of nanocrystals of the stable crystal embedded in a matrix of non-transformed undercooled liquid. The Raman susceptibilities of the undercooled liquid, the GS, and the stable crystal are plotted in Fig. 2. It is observed that the GS has an amorphous-like band-shape. The high resolution of the spectra gives the opportunity to show that the main differences observed between the spectra of the undercooled liquid and the GS (localized by arrows in Fig. 2) correspond to the Raman signatures of the crystal. The spectrum of the GS appears as the envelope of the phonon peaks of the stable crystal. This is the demonstration that the low-frequency Raman spectroscopy is a very suitable technique for the detection and the identification of the earliest stage of crystallization, since the size of nanocrystals, about 30 Å (Derollez et al., 2006; Hedoux et al., 1999), is similar to the unit cell parameters of the crystal (Hernandez et al., 2002).

3. Applications to pharmaceutical materials

The energetic level of a crystalline state or the physical state of APIs, closely connected to the packing and the degree of disorder of the molecules, has considerable consequences on their solubility, bioavailability, and stability during manufacturing processes and during their storage. In this context it is crucial to get information

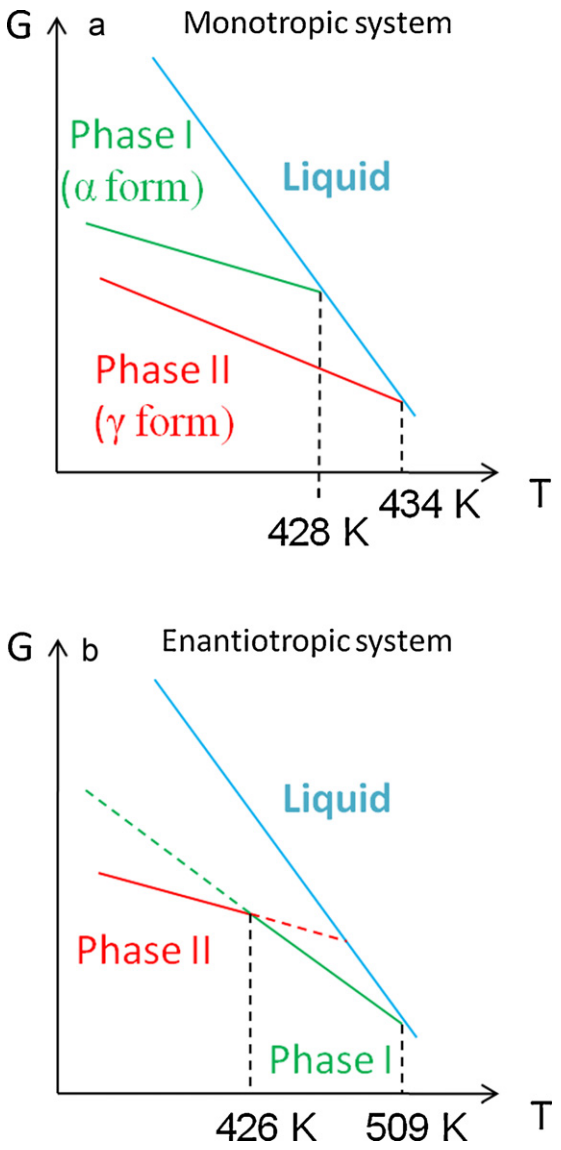

Fig. 3. Typical Gibbs free energy–temperature phase diagrams for (a) a monotropic system corresponding to the G–T diagram of indomethacin and (b) an enantiotropic system corresponding to the G–T diagram of caffeine.

on the structure and dynamics of APIs in relation with the Gibbs energy diagram, in order to predict possible transformations of APIs under different environmental stresses. Indometacin and caffeine are two molecular drugs, characterized by a Gibbs energy diagram distinctive of two different polymorphic situations represented in Fig. 3, corresponding respectively to monotropic and enantiotropic systems.

3.1. Raman investigations in indomethacin

Indomethacin (IMC, 1-(p-chlorobenzoyl)-5-methoxy-2-methylindole-3-acetic acid) is an anti-inflammatory, antipyretic and analgesic drug which exhibits a rich and very original polymorphism characterized by the α–γ monotropic system (Fig. 3a), whose the more stable form is the γ phase (Andronis and Zografi, 2000) which melts at T_m = 434 K (Crowley and Zografi, 2002a). Moreover the more stable phase does not exhibit the highest density, with respect to other crystalline states. Crystal of γ-IMC belongs to the centrosymmetric triclinic space group $P\bar{1}$ with $Z = 2$ (Kistenmacher and Marsh, 1972). The crystal packing is charac-

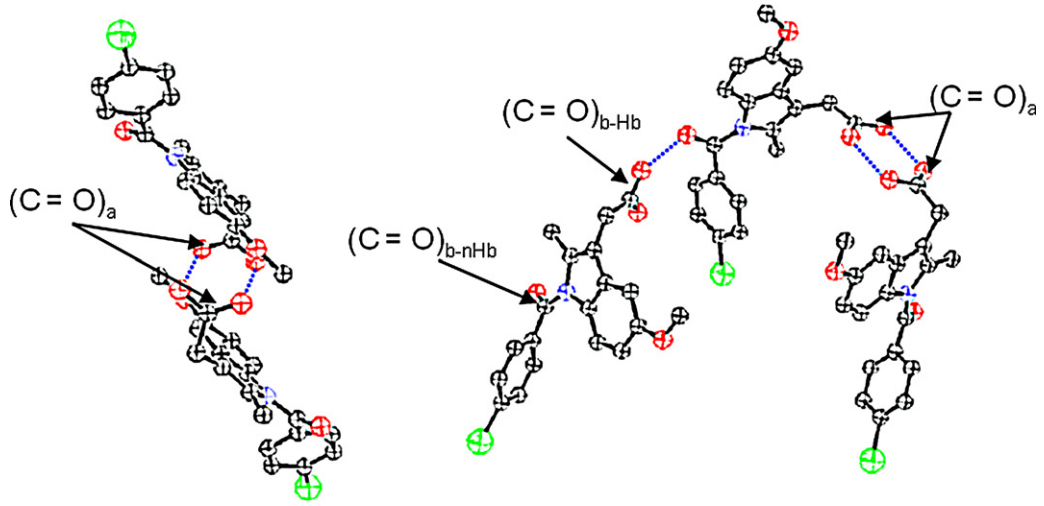

Fig. 4. Molecular associations of indomethacin through hydrogen bonding in dimers and trimers. Characteristic C=O bonds involved in internal vibrations described in Table 1 are localized by arrows.

terized by molecular associations in dimers (Fig. 4) via hydrogen bonding of the carboxylic acid group. The metastable α-phase, obtained by dissolution in methanol and precipitation in water (Kaneniwa et al., 1985), crystallizes in the $P2_1$ space group ($Z=6$) (Chen et al., 2002) and melts at 428 K (Crowley and Zografi, 2002a). The organization in trimers of the α-phase (Fig. 4) is suspected to be at the origin of its higher density (Chen et al., 2002) (1.40) with respect to that of the stable γ-phase (1.38). IMC is known to be a very poor water-soluble drug (Matsumoto and Zografi, 1999), which requires amorphization to enhance oral bioavailability. Grinding is known to be a safe amorphisation method for materials which degrade upon heating or solubilization. However, the method used to prepare the amorphous state has a strong influence on its stability. It is recognized that IMC crystallizes below the glass transition ($T_g = 43\,^{\circ}C$) with different rates of crystallization (Otsuka and Kaneniwa, 1988; Wu and Yu, 2006b), depending on how the amorphous state is prepared. It was reported that melt-quenched amorphous IMC transforms into the most stable γ crystalline state below T_g, and crystallizes toward the metastable α form or toward a mixture of γ and α above T_g (Yoshioka et al., 1994). In this context, the mechanism of amorphization upon pressurizing and grinding, and the crystallization process of the amorphous IMC prepared by grinding can be considered as crucial information to determine and to understand the degree of metastability of amorphous states obtained under different types of stress.

The low-frequency Raman spectra of amorphous and crystalline states of indomethacin are plotted in Fig. 5a. Low-frequency Raman spectra of crystalline states are easily distinguishable from that of the glass since they are composed of phonon peaks corresponding to the lattice vibrations. The LFRS is distinctive of each crystalline form, and the number of Raman active phonons is directly dependent on the degree of symmetry of the crystal. It is clearly observed in Fig. 5, that the degree of symmetry of the metastable α-form is lower than that of γ-IMC. In contrast to the

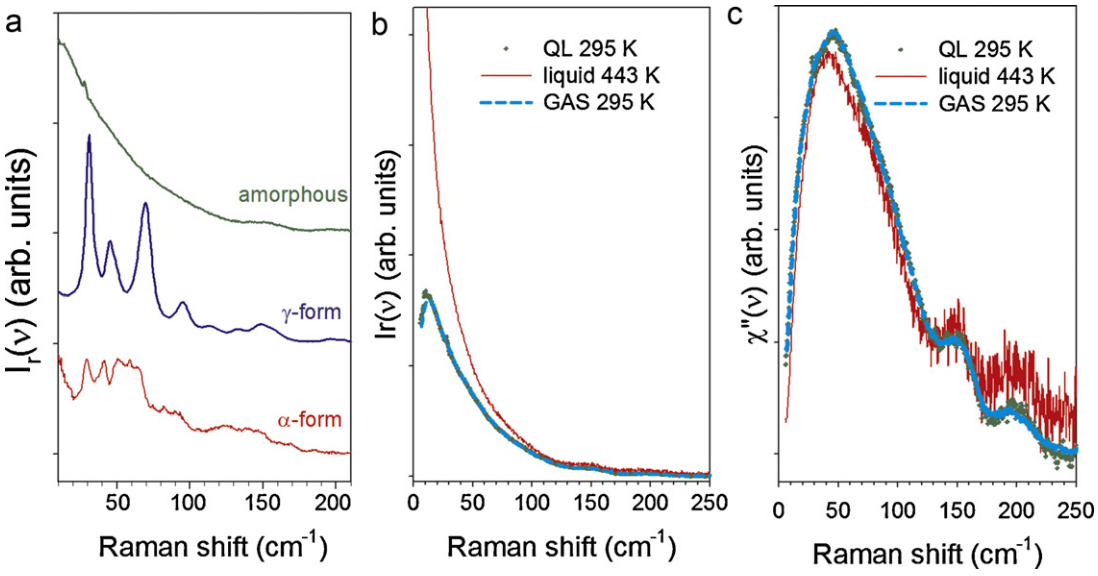

Fig. 5. Representations of the low-frequency spectra in the different states of indomethacin. (a) Reduced intensity in the solid amorphous states (prepared by quench of the liquid and cryogrinding), and in the γ and α crystalline forms at room temperature. (b) Reduced intensity of solid amorphous states at room temperature, obtained by quench of the liquid (QL), and by cryogrinding (GAS), compared to the spectrum of the liquid state recorded at 443 K. (c) Raman susceptibility of amorphous solid states at room temperature (obtained by quench of the liquid and cryogrinding), compared to that of the liquid at 443 K. The conversion of reduced intensity into Raman susceptibility was performed as described in Section 2.2.3.

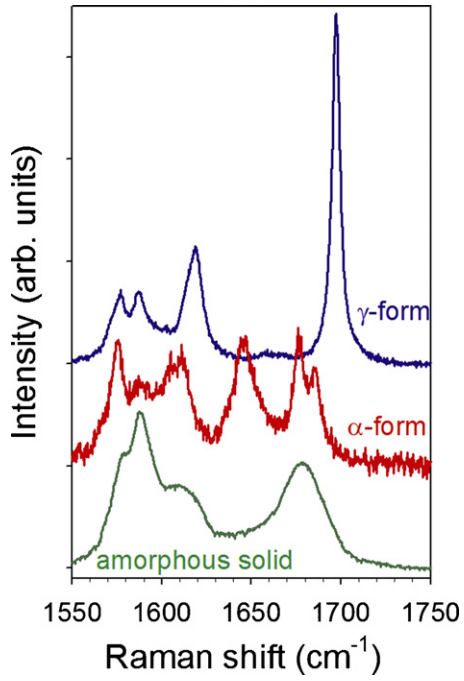

Fig. 6. The Raman spectra of the amorphous solid, α, and γ crystalline forms of indomethacin in the 1550–1750 cm^{-1} range.

crystalline states, no phonon peak is observed in the amorphous state since there is no long-range order. The low-frequency spectrum of vitreous IMC corresponding to the quenched liquid (QL), is only composed of a broad band directly related to the vibrational density of states distinctive of the short-range order, and mainly resulting from an inhomogeneous broadening of phonon peaks. The solid amorphous states, i.e. the quenched liquid (QL) and the cryo-ground powder (GAS) are compared to the liquid in the reduced intensity and Raman susceptibility representations in Fig. 5b and c. The spectra of the solid amorphous states are observed to be superimposed, and the main difference between amorphous solid states and the liquid results from a strong QES component observed in the reduced spectrum of the liquid state. This difference is connected to the important contribution of thermally activated motions at high temperature in the liquid.

The 1550–1750 cm^{-1} region, mainly composed of the C=O stretching (νC=O) bands (Schmidt et al., 2004; Taylor and Zografi, 1997, 1998), was previously determined as very sensitive to molecular associations via hydrogen bonding (Matsumoto and Zografi, 1999; Taylor and Zografi, 1997; Watanabe et al., 2001). The Raman spectrum in this region is distinctive of the different states of IMC (Hedoux et al., 2008), as it can be seen in Fig. 6 for α and γ crystalline forms, and the amorphous state. The assignment of the Raman bands detected in this region in the amorphous state, α and γ forms of IMC is reported in Table 1. Amorphous IMC is considered as mainly composed of cyclic dimers with a too small proportion of H-bonded molecules to form a chain (Taylor and Zografi, 1997), whereas the structure of the γ form is organized in chains of dimers. No Raman band in the C=O stretching region is directly informative of molecular associations via H-bonds between acid groups, both in amorphous state and in the γ form (Taylor and Zografi, 1997). However the bands detected around 1679 cm^{-1} and the 1697 cm^{-1} respectively in the amorphous state and in the γ form, and both assigned to the benzoyl C=O stretching vibration ($\nu(C{=}O)_b$) exhibit a contrasted line-shape depending on the organization of IMC molecules. In the γ form the 1697 cm^{-1} band is influenced by steric hindrance and tension of molecules (Schmidt et al., 2004) imposed by H-bonded associations in dimers. Consequently the frequency and the sharpness of this band reflect the long-range order of dimer chains. This band is distinctive of the γ-form, and its width can be used to probe and to monitor the long-range order in the γ form under different stresses (temperature, pressure, grinding, . . .). In contrast the broadened line-shape of the 1679 cm^{-1} band in the amorphous state (Fig. 6) is probably inherent to the local disorder or to the presence of different molecular conformations and associations, as it was determined in the α form (Chen et al., 2002). As a consequence of the presence of different molecular associations and additional H-bonding, the spectrum of α-IMC is more complex. The (1678 cm^{-1}, 1688 cm^{-1}) doublet was assigned to the H bonded and non-H bonded benzoyl C=O stretching bands, and the Raman band at 1648 cm^{-1} to the C=O stretching vibration of hydrogen bonded acid in agreement with previous studies (Hedoux et al., 2008; Schmidt et al., 2004; Taylor and Zografi, 1997). Consequently, the broad band observed at 1679 cm^{-1} in the amorphous state which appears as the envelope of the 1678 and 1688 cm^{-1} can be interpreted as corresponding to both types (H bonded and non-H bonded) of benzoyl C=O stretching vibrations (Hedoux et al., 2008; Schmidt et al., 2004).

Table 1
Assignment of Raman bands of indomethacin in the 1500–1800 cm^{-1} spectral range.

Raman band (cm^{-1})	Form	Assignment
1588	γ	
1589	Amorphous, α	Ring vibration of indole
1591		
1611	Amorphous, α	
1618	γ	νC=C
1648	α	H bonded acid $\nu(C{=}O)_a$
1678	α	H bonded benzoyl $\nu(C{=}O)_{b\text{-}Hb}$
1679	Amorphous	(Non-H bonded + H bonded) benzoyl $\nu(C{=}O)_b$
1688	α	Non-H bonded benzoyl $\nu(C{=}O)_{b\text{-}nHb}$
1697	γ	Benzoyl $\nu(C{=}O)_b$

3.1.1. Amorphization mechanism by pressurizing and grinding the stable γ form

The 1550–1750 cm^{-1} region was used to monitor the stability and the transformation of γ IMC upon pressurizing and grinding. Fig. 7 shows the evolution of the spectrum at different stages of both amorphization processes. It is clearly observed in Fig. 7a that the 1697 cm^{-1} band is quasi pressure independent upon pressurizing to about 3 GPa contrasting to the other bands in the 1550–1750 cm^{-1} spectral range. This pressure behavior of this band indicates that strong and orientational H-bonding within dimers are responsible for the stability of the γ phase and the poor molecular packing related to the lower density of the γ form compared to that of the α phase. Above 3 GPa, the intensity of the 1697 cm^{-1} band decreases at the expense of a growing band around 1685 cm^{-1}, reflecting the collapse of the dimer chains of the γ-form into a closer packing induced by new molecular associations distinctive of the α-form. Fig. 7a shows that an ordering process (γ → α-like) is observed near 5 GPa, prior to the pressure-induced amorphization corresponding to the disruption of molecular associations. In contrast to the pressure-induced transformation of γ IMC, Fig. 7b shows that for short times of grinding, the intensity of 1697 cm^{-1} decreases at the expense of the broad band located around 1679 cm^{-1} distinctive of the amorphous state. This behavior indicates a disordering process corresponding to the direct disruption of dimer chains into the molecular packing distinctive of the amorphous solid state obtained by undercooling the liquid state. The Raman spectra in the 1550–1750 cm^{-1} region of the shear- and pressure-amorphized solid states plotted in Fig. 7c are different and correspond to two different mechanism of amorphization, leading to two different amorphous states associated with distinctive

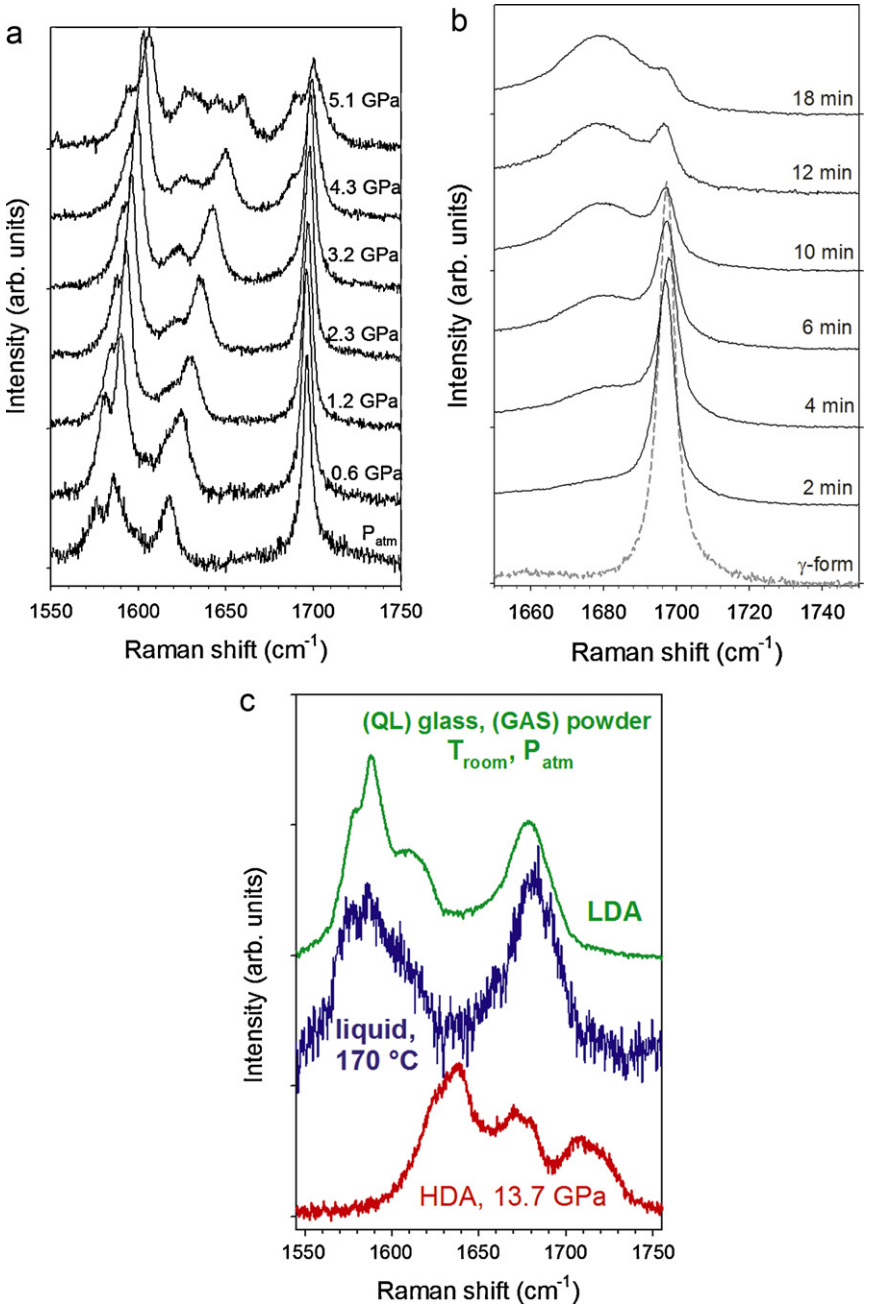

Fig. 7. Influence of pressurizing and grinding on the Raman spectrum of indomethacin in the 1550–1750 cm^{-1} range. (a) Raman spectra at different stages of pressurizing the γ form. (b) Raman spectra at different stages of cryogrinding the γ form. (c) Comparison between Raman spectra in different amorphous states; liquid state obtained by heating, solid low-density amorphous (LDA) state obtained by quench of the liquid or cryogrinding, and high-density amorphous (HAD) state obtained upon pressuring the γ form up to 13.7 GPa.

spectra. Pressure-induced amorphization of γ-IMC can be considered as a density-driven transformation, which can be described as a two-step transformation. (i) an ordering process corresponding to the formation of additional H-bonding and new molecular associations characterized by a denser packing similar to that of α form (as expected from Le Chatelier's principle), prior to (ii) a disordering process leading to a high density amorphous (HDA) state upon further pressurizing. In contrast to pressurization, grinding directly induces disordering, i.e. the disruption of low-density dimer chains leading to the loss of the long-range order at the expense of a low-density amorphous (LDA) state characterized by a molecular packing similar to that of the liquid. Indeed, the spectrum of the liquid state appears as the envelope of the spectra of the quenched liquid or the ground powder corresponding to the low-density state. It is worth noting that the amorphization by grinding is not a consequence of successive local melting due to hot spots generated by the mechanical shocks, as frequently suggested. Indeed, Raman investigations on D-glucose (Dujardin et al., 2008) have shown that the glassy state prepared by ball milling was free of mutarotation, whatever the starting glucose variety (α or β), while mutarotaion is unavoidable using the usual thermal quench of liquid, in agreement with other examples (Willart and Descamps, 2008).

The LFRS gives complementary information about the long-range order during the amorphization processes. The pressure dependence of the LFRS of γ IMC is plotted in Fig. 8a. This figure shows a strong pressure dependence of the phonon frequencies, and confirms the ordering process into a denser phase, observed

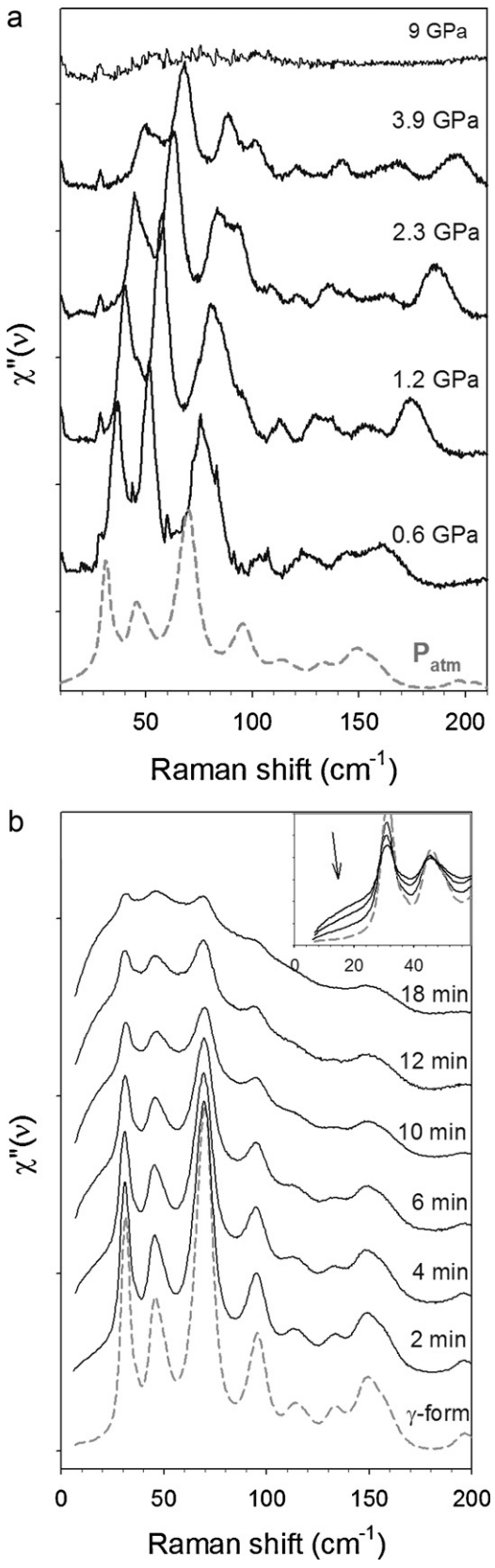

Fig. 8. Evolution of the Raman susceptibility at different stages of solid amorphization from the γ form of indomethacin. (a) Upon pressurizing. (b) Upon grinding; Raman spectra corresponding to 0, 2, 4 and 6 min of cryogrnding are superpimposed in the inset. The arrow points out the enhancement of Raman susceptibility distinctive of the volume fraction of amorphous matter.

at higher frequencies in Fig. 7a. For the high pressures, the phonon peaks flatten and cannot be detected above 9 GPa. The Raman susceptibility is plotted at different stages of shear amorphization in Fig. 8b. An enhancement of the susceptibility is clearly observed at the low frequencies corresponding to the BP, and the phonon peaks of the γ form broaden as the time of grinding increases. This indicates that the disruption of dimer chains observed at higher frequencies leads to amorphization and to lattice distortions in the non-amorphized crystals. Fig. 8b reveals the high sensitivity of the LFRS to detect a small amount of amorphous matter in a crystalline matrix, through the enhancement of the susceptibility at very low frequencies (see the inset of Fig. 8b) detected after 2 min of grinding and corresponding to shear-amorphized crystals. Using a quantification method based on the LFRS analysis, less than 2% of amorphous contents can be detected for indomethacin. Amorphization can be suspected at higher frequencies in Fig. 7b, through the emergence of a very broad and weak intensity around 1670 cm^{-1} which can not give a significant quantification of the amorphous matter. It was shown that chemometric FT-Raman spectroscopy allows the determination of 2% of amorphous or crystalline material in IMC (Okumura and Otsuka, 2005). This value can be determined from the analysis of the fingerprint region, mainly because of the high sensitivity of the 1697 cm^{-1} band to the long-range order in the γ form.

The analysis of both routes of amorphization points out that the dimer associations through hydrogen bonding are responsible for the stability of the γ form, while the mechanism of amorphization (ordering or disordering process) depends on the type (tensile or shearing) of stress. The capability to form different amorphous states prepared by distinct routes is recognized as a general property of polyamorphic systems (Wilding et al., 2006), suggesting the existence of a first-order transition between the two different amorphous solid states in indomethacin, as observed in water (Bosio et al., 1986; Mishima et al., 1984, 1985). Moreover, the stable γ form of indomethacin is characterized by a low-density packing inherent to strong orientational hydrogen bonds, as observed for hexagonal ice. The possibility of obtaining different amorphous structures gives the opportunity to optimize bioavailability, and stabilization procedures.

3.1.2. Crystallization of ground amorphous powder

The analysis of the early stages of crystallization can be considered as a tool for insight into the amorphous state, especially to describe local structures or molecular packing. It was demonstrated that the LFRS is also very sensitive to detect, to identify and to quantify a very low content of crystalline matter in a matrix of amorphous solid or liquid. The Raman spectra of the amorphous powder obtained by cryogenic grinding were recorded at room temperature in the low-frequency range and in the C=O stretching region in order to analyze the stability of the ground amorphous powder. The Raman spectra are plotted in Fig. 9a and b in the early stages of transformation. The analysis of both figures reveals that the low-frequency range is more sensitive to the detection of crystallization traces toward the γ form, than the C=O stretching region, through the observation of a subtle shoulder (see the arrow in Fig. 9a) corresponding to an intense phonon peak of the γ phase. The method usually used to detect and determine the degree of crystallinity in a matrix of amorphous IMC (Schmidt et al., 2004; Taylor and Zografi, 1998) was based on the ratio of intensities of the 1679 cm^{-1} band (in the spectrum of the amorphous state) and the 1697 cm^{-1} band (in the spectrum of the γ crystalline form). It is clear that the accuracy of this method is limited by the difficulties to fit the shoulder of the broad 1679 cm^{-1} band, for a low degree of crystallinity. Same difficulties occur to fit a very flat and broad band tailing the low-frequency side of the sharp and intense 1698 cm^{-1} band, for a high degree of crystallinity. In the LFRS, the fraction

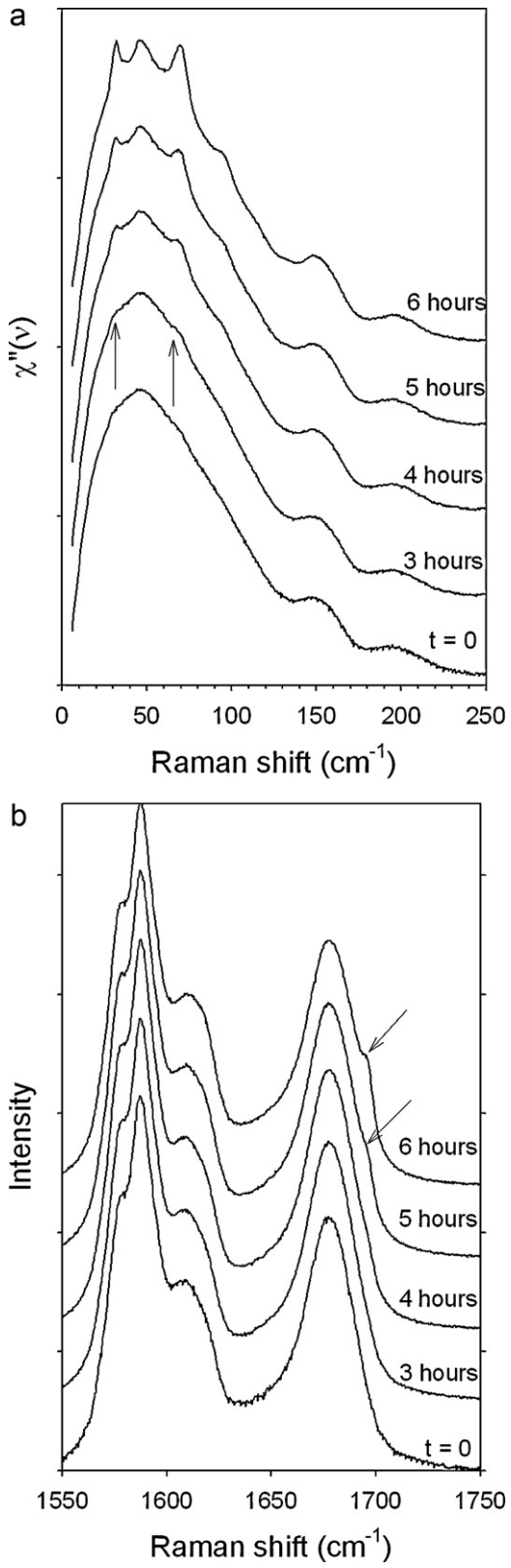

Fig. 9. Evolution of the Raman spectrum of ground amorphous powder at room temperature (a) in the low-frequency range, (b) in the 1550–1750 cm^{-1} range and (c) the arrows localize the first traces of crystallization in both spectral ranges.

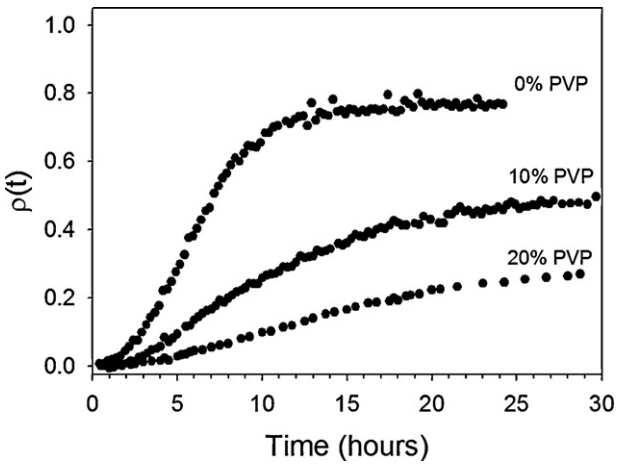

Fig. 10. Time evolution of the volume fraction of γ-IMC crystal in the absence and in the presence of PVP.

($\rho(t)$) of the γ phase isothermally transformed was evaluated from the integration of the spectrum difference between 62 cm^{-1} and 77 cm^{-1}, according to

$$\rho(t) = \frac{\int_{62\,cm^{-1}}^{77\,cm^{-1}} \chi''(t) - \int_{62\,cm^{-1}}^{77\,cm^{-1}} \chi''(t=0)}{\int_{62\,cm^{-1}}^{77\,cm^{-1}} \chi''(t_{end}) - \int_{62\,cm^{-1}}^{77\,cm^{-1}} \chi''(t=0)} \quad (7)$$

where χ"(t = 0), χ"(t_{end}), and χ"(t) are the Raman susceptibilities of the amorphous state, the γ form and the partially crystallized state. The domain of integration corresponds to the frequency range where the most intense phonon peak of γ form is detected. The time dependence $\rho(t)$, plotted in Fig. 10, has a clear sigmoidal shape. This experiment indicates that the GAS IMC systematically and rapidly crystallizes into the γ form at room temperature, i.e. at $T_g - 20$ K, and the degree of crystallization slowly increases after 12 h. The sigmoidal shape of $\rho(t)$ seems to indicate that the crystallization will not be completed since a residual and significant fraction (∼20%) of amorphous powder is clearly detected. Crystallization kinetics was analyzed (Hédoux et al., 2009) using the Kolmogorov–Johnson–Mehl–Avrami (KJMA) equation (Jou and Lusk, 1997; Price, 1990):

$$\rho(t) = 1 - \exp\left[-k(t - t_0)^n\right] \quad (8)$$

where $\rho(t)$ represents the fraction crystallized at time t, t_0 is the induction time, k is a constant dependent on the nucleation and growth rate, and n is a constant reflecting the dimension of crystallization (Crowley and Zografi, 2002a,b; Jou and Lusk, 1997; Price, 1990). The low value obtained for n (∼2) was interpreted as the signature of a site-saturation with a two-dimensional growth (Hédoux et al., 2009; Jou and Lusk, 1997), suggesting that a number of nuclei are prepared initially in a ground amorphous sample.

3.1.3. *Influence of polyvinylpyrrolidone (PVP) on ground amorphous IMC*

It is well known that solid dispersions of PVP and IMC using different techniques inhibits crystallization of amorphous IMC (Shakhtshneider et al., 2007; Taylor and Zografi, 1997). From IR and FT-Raman in the 1500–1800 cm^{-1} range, it was shown that in solid dispersions of PVP and IMC prepared using a solvent evaporation technique (Taylor and Zografi, 1997) or using melt extrusion (Forster et al., 2001), IMC interacts with PVP. Interactions correspond to hydrogen bonds formed between the drug hydroxyl and polymer carbonyl resulting in disruption of IMC dimers, and then in inhibition of crystallization into γ form. It was shown that drug/PVP glass solutions can also be obtained by grinding (Balani et al., 2010;

Shakhtshneider et al., 2007). Re-crystallization of IMC was analyzed at room temperature in the presence of PVP, from low-frequency Raman investigations and the evolution of the volume fraction $\rho(t)$ is plotted in Fig. 10 for different PVP concentrations. Fig. 10 confirms that crystallization of IMC is inhibited with the addition of a weak concentration of PVP, as observed for solid dispersions prepared by other methods. However, in contrast to solid dispersions prepared using solvent evaporation or extrusion methods, it was shown (Shakhtshneider et al., 2007) that the Raman spectra in the 1550–1750 cm^{-1} of glassy mixtures obtained by grinding and spectra of physical mixtures were similar for PVP concentrations ranging between 20% and 80%. Raman spectra of amorphous mixtures prepared by cryogrinding were plotted in Fig. 11 for different concentrations of PVP. It is clearly observed in Fig. 11a that $\chi''(\nu)$ spectra are similar for concentrations up to 50%. Above 50% the VDOS of IMC is significantly broadened by a tail in the high-frequency side of the low-frequency band corresponding to the contribution of the VDOS of PVP. It is worth noting that the glass transition temperature of IMC–PVP cryoground mixtures significantly increases for PVP concentrations higher than 50% (Shakhtshneider et al., 2007). No significant change of the Raman band-shape can be detected in the 1500–1800 cm^{-1} range plotted in Fig. 11b, suggesting no direct interaction between IMC and PVP through hydrogen bonding. These investigations suggest that crystallization inhibition in IMC-PVP cryoground mixtures could be related to a partitioning effect of PVP, preventing the growth of γ nuclei.

3.2. Raman spectroscopy investigations in caffeine

Caffeine ($C_8H_{10}N_4O_2$) is a well-known agrochemical and therapeutic agent. Anhydrous caffeine is known to occur in two different polymorphic phases (called I and II) which constitute an enantiotropic system (Bothe and Cammenga, 1979) (Fig. 3b). The commercial form (II) is thermodynamically stable at room temperature and transforms upon heating at 153 °C (Cesaro and Starec, 1980) into form I which is characterized as a disordered crystalline state from calorimetric and X-ray investigations (Cesaro and Starec, 1980; Derollez et al., 2005). This state can be maintained at low-temperature in a very slowly relaxing metastable situation. The I → II transformation is hindered at room temperature (Lehto and Laine, 1998) but kinetics of transformation are significantly faster around 90 °C. Dielectric (Descamps et al., 2005) and X-ray (Derollez et al., 2005) investigations in the undercooled form I have revealed that this metastable form is a dynamically and orientationally disordered state i.e. a rotator phase also called plastic crystal. The purified sample which is in the metastable form I, was firstly heated in the temperature domain of faster transformation (90 °C), and maintained at this temperature for the analysis of the isothermal dependence of the Raman spectrum in the low-frequency range (10–600 cm^{-1}), and in the fingerprint region lying between 600 cm^{-1} and 1800 cm^{-1}. Raman susceptibilities in the low-frequency region (10–100 cm^{-1}) of the metastable state of form I at the beginning of the isothermal transformation ($t = 0$) and in a state close to the form II after about 32 h of transformation are plotted in Fig. 12. These spectra are compared to that of the non purified sample at 90 °C, considered as mostly in phase II. Fig. 13 is divided in two spectral ranges corresponding to the lattice mode (10–100 cm^{-1}) and the internal vibration (100–600 cm^{-1}) regions. The low-frequency region exhibits significant changes during the isothermal transformation, while above 100 cm^{-1} the spectra of internal modes are rigorously superimposed. No phonon peak can be distinguished in the Raman susceptibility of the phase (I). Such a band shape for the low-frequency spectrum reflects a high degree of disorder as observed in the crystalline rotator phase (Affouard et al., 2001; Denicourt et al., 2003; Rolland and Sauvajol, 1986), in agreement with previous investigations suggesting the existence

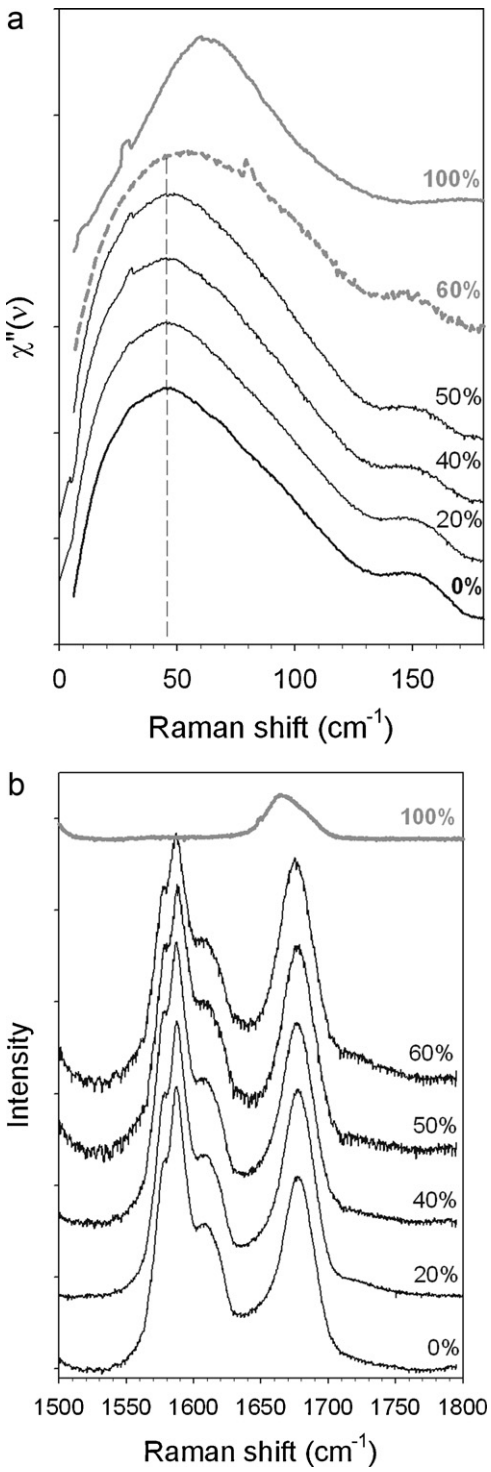

Fig. 11. Raman spectra at room temperature of solid amorphous IMC–PVP mixtures prepared by cryogrinding (a) in the low-frequency range and (b) in the 1500–1800 cm^{-1} range.

of a dynamical orientational disorder in phase (I) (Descamps et al., 2005). In rotator phases the mass centers of molecules generate a periodic lattice, i.e. a crystal, but the orientational disorder of molecules induces the absence of periodicity for atoms. In this case, $G(\nu)$ represents the librational density of states, and is related to the distribution of frequencies experienced by a central molecule located in different molecular environments. It is worth noting the amorphous-like band-shape of the LFRS although the physical state is really crystalline.

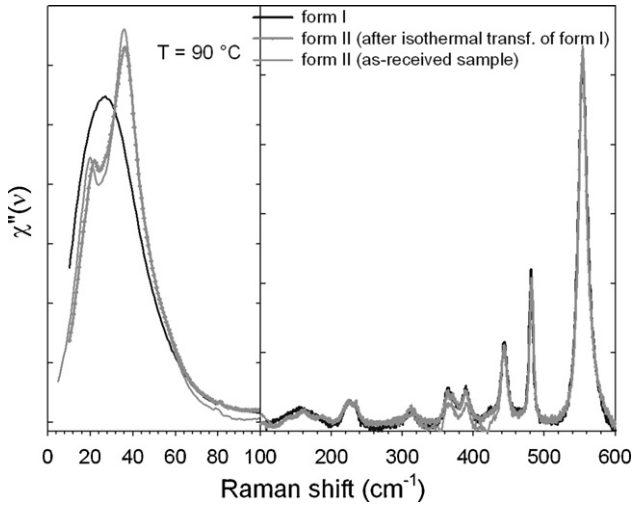

Fig. 12. Raman susceptibility of the two crystalline forms in caffeine. The spectrum is divided in two windows corresponding to the lattice mode region (10–100 cm^{-1}) and the internal mode region (above 100 cm^{-1}).

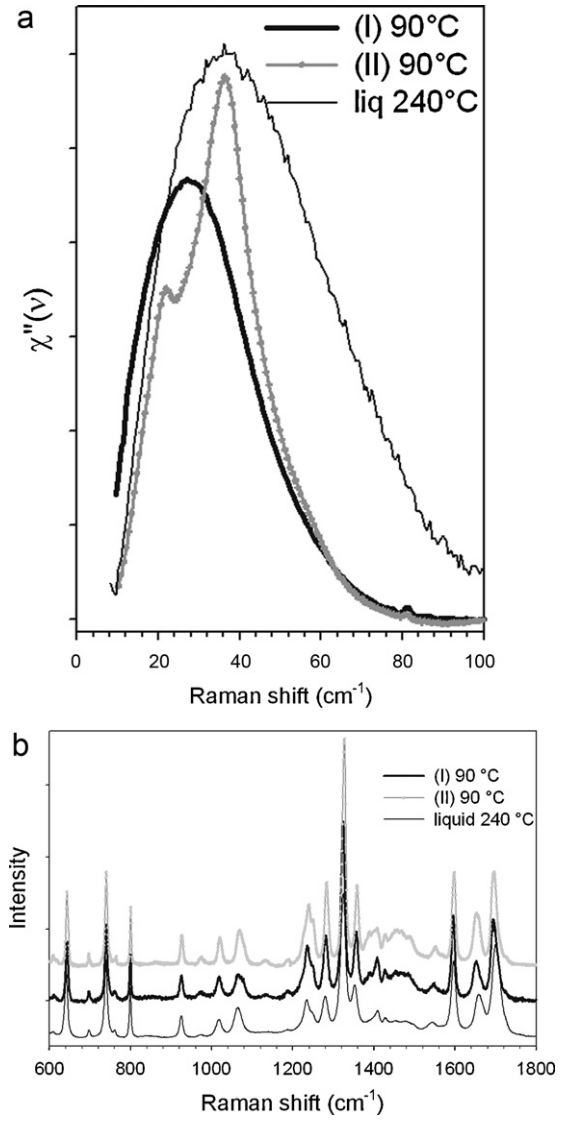

Fig. 13. Representations of the Raman spectrum of crystalline (forms I and II) and liquid states (a) in the low-frequency range: Raman susceptibility and (b) in the fingerprint region: Raman intensity.

The Raman susceptibility in phase (II) is easily distinguishable from that of phase (I). It is dominated by a double hump which appears as a splitting of the broad band observed in the spectrum of phase (I). Both low-frequency bands are too broad be considered as two phonon peaks, reflecting a significant degree of disorder of the stable phase. It is observed that the spectrum of the non purified sample is slightly different from that obtained after the isothermal transformation, indicating that the transformation into the form II is not complete.

In the 100–600 cm^{-1} frequency range the Raman spectra of both crystalline forms are superimposed, indicating that no ordering process can be detected in this frequency range. The spectra of both forms of crystalline caffeine are compared to that of the liquid state in the low-frequency and the fingerprint regions respectively plotted in Fig. 13a and b. In contrast to the LFRS where the different states of caffeine are clearly distinguishable, the Raman spectra are very similar in the internal mode region. This is the evidence of a disordered molecular environment in forms I and II, suggesting a similar arrangement of the molecular centers of mass and an analogous orientationally disorder in both crystalline phases which is reminiscent of the local order in the liquid state. Both low and high-frequency investigations of the different states of caffeine are converging into the description of form II of caffeine as a rotator phase. The splitting of the broad low-frequency band in form I into two broad components in form II could be related to the tilt of the molecular plane out of the hexagonal (a,b) plane of form I, as determined from X-ray investigations (Enright et al., 2007; Lehmann and Stowasser, 2007). This study shows the capabilities of Raman spectroscopy to give the clear evidence of disorder in form II, reflecting an original polymorphism in caffeine. In previous works (Hedoux et al., 2001b; Hédoux et al., 2009), it was shown that the integrated intensity of low-frequency Raman signatures of a growing phase could be related to a degree of transformation. The reduced intensity was integrated between 30 cm^{-1} and 45 cm^{-1}, where a shoulder is observed to grow during the isothermal transformation I → II. The degree of this transformation is determined from the relation:

$$\rho(t) = \frac{\int_{80cm^{-1}}^{45cm^{-1}} I_r(t) - I_r(t=0)}{\int_{80cm^{-1}}^{45cm^{-1}} I_r(t_{end}) - I_r(t=0)} \quad (9)$$

where t_{end} is the time of complete transformation. The spectrum of the as-received (non purified) sample at 90 °C was used to determine the integrated intensity at t_{end}, since it is considered as mainly in form II. The time dependence of this degree of transformation is reported in Fig. 14. This figure reveals that the kinetics is very fast at the earliest stage of transformation, and becomes very slow at longer times. The experimental ρ(t)-curve was fitted using the Avrami-like function $\rho(t) = 1 - \exp[-(t/\tau)^n]$. The fitting procedure leads the exponent $n \approx 0.7$, associated with an atypical stretched exponential law for nucleation and growth process which is generally characterized by a sigmoidal shape. The kinetics law is similar to that obtained from dielectric experiments (Decroix et al., 2008), and has been interpreted from the consideration that the isothermal transformation is driven by a slow nucleation in grains characterized by a distribution of their size ranging below the characteristic dimension of nucleation and growth process (Decroix et al., 2008).

3.3. Micro Raman spectroscopy

It was recently demonstrated that Micro Raman spectroscopy (MRS) gives detailed descriptions of coexisting phases in first-order phase transformations (Hédoux et al., 2006), and thus brings out information on the mechanism of transformation. In the general context of developing advanced pharmaceutical dosage forms, MRS

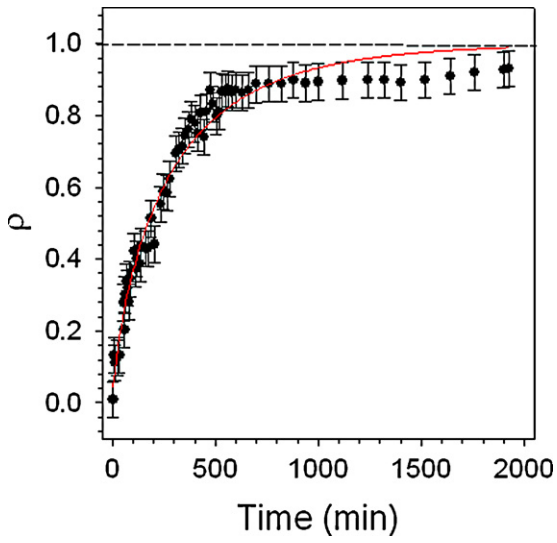

Fig. 14. Evolution of the volume of transformed fraction from form I into form II of caffeine during an isothermal ageing at 90 °C.

could be a useful tool. In the drug delivery systems, MRS can be used to describe the drug distribution into the polymeric membrane, and the physical state of the coating in order to understand the underlying drug release mechanism from pellets coated with aqueous polymer dispersions. This kind of information could be important to understand the drug release rate under different preparations of dosage forms (Yang et al., 2010). Lipid implants can be used as time-controlled protein delivery systems (Guse et al., 2006). In this case pharmaceutical proteins must be stabilized in their native state over prolonged periods of time to achieve therapeutic effects. Consequently, lysozyme-loaded implants are freeze-dried, since freeze-drying is recognized to be a common procedure to stabilize the native state of labile protein in a dried solid state. Implant preparation and freeze-drying procedures are both sources of protein denaturation. Raman spectroscopy is recognized as a probe of the secondary structure (Williams and Dunjer, 1981), and can be used for monitoring the protein denaturation (Hedoux et al., 2006). MRS gives the opportunity to analyze the conformation and the distribution of the protein within the lipidic implant. We report in Fig. 15 first investigations in lysozyme-loaded lipid implants (unpublished data). It is observed that lysozyme (white region) is in its native conformation, despite its exposition to various sources of stress during the preparation of the implant. However, it is not homogeneously distributed in the triglyceride matrix, with a significant concentration in channels by which water is removed during the drying stages in the freeze-drying procedure. Consequently, it is very likely that MRS is an important tool for the understanding of the release mechanisms of the API in drug delivery systems.

4. Concluding remarks

We have reported investigations carried out on indomethacin and caffeine to show the important contribution of the low-frequency Raman spectrum to describe and to understand the mechanism of phase transformation in two different polymorphic situations. It was demonstrated that the LFRS is very suitable for the detection and quantification of small amorphous or crystalline contents. The analysis of caffeine gives the demonstration that the LFRS is a crucial tool to investigate the mechanism of phase transformation in disordered polymorphs. Investigations in the fingerprint region are consistent with the description of form II of caffeine as orientationally disordered, with a local order very similar to that of form I and the liquid state. It is also demonstrated that the fingerprint region can not be systematically used for the determination of small amorphous or crystalline contents from chemometric method (Okumura and Otsuka, 2005) for the quantitative analysis of polymorphic mixtures from principal components analysis (Strachan et al., 2004), especially in the case of the absence of sensitive Raman signatures of the physical states or crystalline forms.

On the other hand, Raman investigations in the high frequency range (internal vibrations) can provide information on subtle conformational changes, such as mutarotation of glucose (Dujardin et al., 2008), without low-frequency signatures. Raman spectra of amorphous milled α and β forms of glucose are plotted in the 5–600 cm^{-1} range in Fig. 16 and compared with that of the quenched liquid. It is clearly observed that spectra are superimposed in the 10–200 cm^{-1} low-frequency range, while the spectra can be easily distinguished above 200 cm^{-1}, reflecting similar collective motions despite of different molecular conformations associated with different internal vibrations. The similarity between the low-frequency spectra for the amorphous states pre-

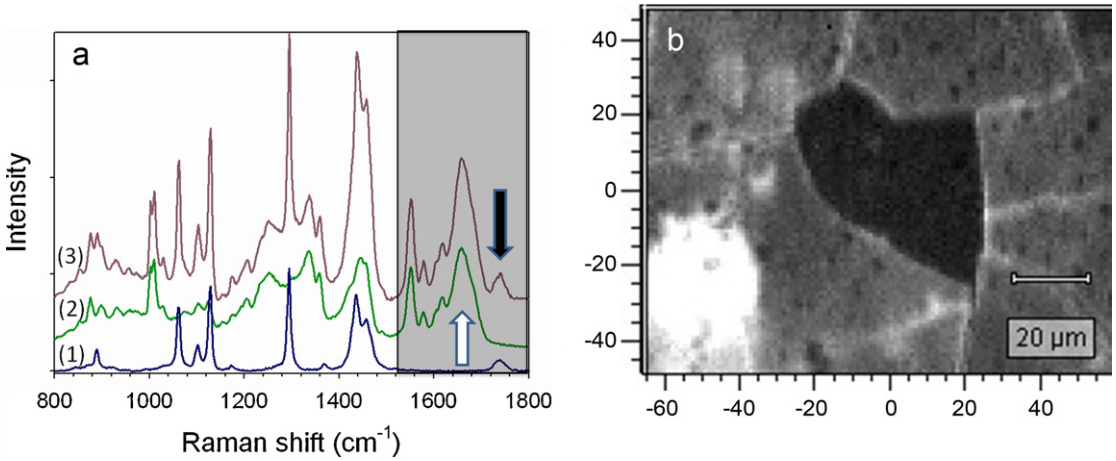

Fig. 15. Description of the method for obtaining a mapping of a transverse section of cylindrical lysozyme-loaded lipid implants. (a) The fingerprint spectrum of matrices which consist of triglycerides (1), and lysozyme (2) separately recorded, and the spectrum of mixed lysozyme/triglyceride (3) recorded in the lysozyme-loaded lipid implant; the arrow localizes the Raman band used to detect triglyceride (black arrow) and lysozyme (white arrow, corresponding to the amide I band). The grey area indicates the spectral region used for the mapping. (b) Raman mapping of a transverse section of cylindrical lysozyme-loaded lipidic implants. Grey regions correspond to the homogeneous distribution of lysozyme in the matrix, while white or black regions indicate the major presence of lysozyme or triglecyride. White strings indicate the presence of lysozyme in the channels induced by water removing during the freeze-drying process. This Raman image was calculated from 10146 spectra recorded in the 1500–1800 cm^{-1} region.

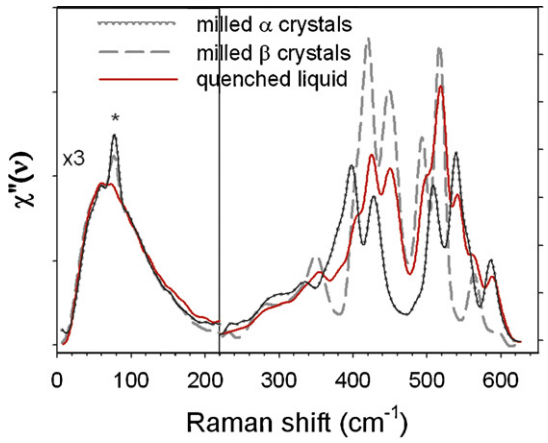

Fig. 16. Raman susceptibility spectra at room temperature of amorphous glucose prepared by quench of the liquid, initially crystalline α form milled for 14 h at −15 °C, and initially crystalline β form milled for 14 h at −15 °C; the star localizes a laser band. The Raman susceptibility was multiplied by 3 in the 0–220 cm^{-1} to give a better description of the vibrational density of states in the different amorphous states of glucose.

pared by milling α and β forms is consistent with the close description of the long-range order in the two corresponding crystalline phases (Chu and Jeffrey, 1968; Ferrier, 1960; McDonald and Beevers, 1952). It is worth noting that the spectrum of the quenched liquid corresponds to the envelope of the spectra α and β amorphous states, indicating that the quenched liquid is a mixture of the two anomers.

This paper brings out the capabilities of Raman spectroscopy to give a precise structural description in organic molecular material, from the molecular conformation to the molecular packing in crystalline state as well as in highly disordered states (glassy, liquid states or plastic crystals).

Acknowledgements

The authors are indebted to L. Paccou, J.-F. Willart, N. Dujardin, A.-A. Decroix, E. Dudognon, J. Dutet, S. Krenzlin and Professor J. Siepmann for their contribution to the reported investigations.

References

Achibat, T., Boukenter, A., Duval, E., 1993. Correlation effects on Raman scattering from low-energy vibrational modes in glasses. II. Experimental results. Journal of Chemical Physics 99, 2046–2051.
Affouard, F., Hédoux, A., Guinet, Y., Denicourt, T., Descamps, M., 2001. Indication for a change of dynamics in plastic crystal chloroadamantane: Raman scattering experiment and molecular dynamics simulation. Journal of Physics Condensed Matter 13, 355011–355014.
Andronis, V., Zografi, G., 2000. Crystal nucleation and growth of indomethacin polymorphs from the amorphous state. Journal of Non Crystalline Solids 271, 236–248.
Angell, C.A., 1991. Relaxation in liquids, polymers and plastic crystals – strong/fragile patterns and problems. Journal of Non-Crystalline Solids 131–133, 13–31.
Bahl, D., Bogner, R., 2006. Amorphization of indomethacin by co-grinding with neusilin: amorphization kinetics, physical stability and mechanism. Pharmaceutical Research 23, 2317–2325.
Balani, P.N., Wong, S.Y., Ng, W.K., Widaja, E., Tan, R.B.H., Chan, S.Y., 2010. Influence of polymer content on stabilizing milled amorphous salbutamol sulfate. International Journal of Pharmaceutics 391, 125–136.
Boldyreva, E.V., 2007. High-pressure diffraction studies of molecular organic solids. A personal view. Acta Crystallographica A64, 218–231.
Boldyreva, E.V., Shakhtshneider, T.P., Ahsbahs, H., Sowa, H., Uchtmann, H., 2002. Effect of high pressure on the polymorphs of paracetamol. Journal of Thermal Analysis and Calorimetry 68, 437–452.
Boldyreva, E.V., Dmitriev, V., Hancock, B., 2006. Effect of pressure up to 5.5 GPa on dry powder samples of chlorpropamide form-A. International Journal of Pharmaceutics 327, 51–58.
Bosio, L., Johari, G.P., Teixeira, J., 1986. X-ray study of high-density amorphous water. Physical Review Letters 56, 460–463.
Bothe, H., Cammenga, H.K., 1979. Phase transitions and thermodynamic properties of anhydrous caffeine. Journal of Thermal Analysis 16, 267–275.
Breitenbach, J., Schrof, W., Neumann, J., 1999. Confocal Raman-spectroscopy: analytical approach to solid dispersions and mapping of drugs. Pharmaceutical Research 16, 1109–1113.
Cesaro, A., Starec, G., 1980. Thermodynamic properties of caffeine crystal forms. Journal of Physical Chemistry 84, 1345–1346.
Chan, H.K., Doelker, E., 1985. Polymorphic transformation of some drugs under compression. Drug Development and Industrial Pharmacy 11, 315–332.
Chen, X., Morris, K.R., Griesser, U.J., Byrn, S.R., Stowell, J.G., 2002. Reactivity differences of indomethacin solid forms with ammonia gas. Journal of the American Chemical Society 124, 15012–15019.
Chieng, N., Rehder, S., Saville, D., Rades, T., Aaltonen, J., 2009. Quantitative solid-state analysis of three solid forms of ranitidine hydrochloride in ternary mixtures using Raman spectroscopy and X-ray powder diffraction. Journal of Pharmaceutical and Biomedical Analysis 49, 18–25.
Chu, S.S.C., Jeffrey, G.A., 1968. The refinement of the crystal structures of beta-D-glucose and cellobiose. Acta Crystallographica B24, 830–838.
Crowley, K.J., Zografi, G., 2002a. Cryogenic grinding of indomethacin polymorphs and solvates: assessment of amorphous phase formation and amorphous phase physical stability. Journal of pharmaceutical sciences 91, 492–507.
Crowley, K.J., Zografi, G., 2002b. Water vapor absorption into amorphous hydrophobic drug/poly(vinylpyrrolidone) dispersions. Journal of Pharmaceutical Sciences 91, 2150–2165.
Decroix, A.-A., Carpentier, L., Descamps, M., 2008. Time-resolved dielectric investigation of relaxation kinetics in metastable caffeine. Philosophical Magazine 88, 3925–3930.
Denicourt, T., Hedoux, A., Guinet, Y., Willart, J.F., Descamps, M., 2003. Raman scattering investigations of the stable and metastable phases of cyanoadamantane glassy crystal. Journal of Physical Chemistry B 107, 8629–8636.
Derollez, P., Correia, N., Danede, F., Affouard, F., Lefebvre, J., Descamps, M., 2005. Ab initio structure determination of the high-temperature phase of anhydrous caffeine by X-ray powder diffraction. Acta Crystallographica B61, 329–334.
Derollez, P., Hédoux, A., Guinet, Y., Lefebvre, J., Descamps, M., Hernandez, O., 2006. Micro(nano)structure of the glacial state in triphenyl phosphite. Zeitschrift für Kristallographie Supplement 23, 557–562.
Descamps, M., Correia, N., Derollez, P., Danede, F., Capet, F., 2005. Plastic and glassy crystal states of caffeine. Journal of Physical Chemistry B109, 16092–16098.
Descamps, M., Willart, J.F., Dudognon, E., 2006. Non equilibrium transformations of molecular compounds induced mechanically. AIP Conference Proceedings. Flow Dynamics: The Second Conference on Flow Dynamics 832, 56–63.
Dujardin, N., Willart, J.-F., Dudognon, E., Hédoux, A., Guinet, Y., Paccou, L., Chazallon, B., Descamps, M., 2008. Solid state vitrification of alpha and beta D-glucose by mechanical milling. Solid State Communications 148, 78–82.
Duval, E., Boukenter, A., Achibat, T., 1990. Vibrational dynamics and the structure of glasses. Journal of Physics: Condensed Matter 2, 10227–10234.
Enright, G., Terskikh, V., Brouwer, D., Rpmeester, J., 2007. The structure of two anhydrous polymorphs of caffeine from single-crystal diffraction and ultrahigh-field solid-state C NMR spectroscopy. Crystal Growth and Design 7, 1406–1410.
Fabiani, F., Allan, D., Dawson, A., David, W., McGregor, P., Oswald, I., Parsons, S., Pulham, C., 2003. Pressure-induced formation of a solvate of paracetamol. Chemical Communication 24, 3004–3005.
Fabiani, F., Allan, D., David, W., Davidson, A., Lennie, A., Parsons, S., Pulham, C., Warren, J., 2007. High-pressure behavior of pharmaceuticals: an exploration of the behavior of Piracetam. Crystal Growth and Design 7, 1115–1124.
Fabiani, F., Pulham, C., 2006. High-pressure studies of pharmaceutical compounds and energetic materials. Chemical Society Reviews 35, 932–942.
Ferrier, W.G., 1960. The crystal structure of beta-D-glucose. Acta Crystallographica 13, 678–679.
Forster, A., Hempenstall, J., Rades, T., 2001. Investigations of drug/polymer interaction in glass solutions prepared by melt extrusion. The Internet Journal of Vibrational Spectroscopy 5, 6–20.
Galeener, F.L., Sen, P.N., 1978. Theory for the first-order vibrational spectra of disordered solids. Physical Review B 17, 1928–1933.
Guse, C., Koennings, S., Kreye, F., Siepmann, F., Goepferich, A., Siepmann, J., 2006. Drug release from lipid-based implants: elucidation of the underlying mass transport mechanisms. International Journal of Pharmaceutics 314, 137–144.
Ha, A., Cohen, I., Zhao, X., Lee, M., Kivelson, D., 1996. Supercooled liquids and polyamorphism. Journal of Physical Chemistry 100, 1–4.
Hedoux, A., Guinet, Y., Descamps, M., 1998. Raman signature of polyamorphism in triphenyl phosphite. Physical Review B Condensed Matter 58, 31–34.
Hedoux, A., Hernandez, O., Lefebvre, J., Guinet, Y., Descamps, M., 1999. Mesoscopic description of the glacial state in triphenyl phosphite from an X-ray diffraction experiment. Physical Review B Condensed Matter 60, 9390–9395.
Hedoux, A., Derollez, P., Guinet, Y., Dianoux, A.J., Descamps, M., 2001a. Low-frequency vibrational excitations in the amorphous and crystalline states of triphenyl phosphite: a neutron and Raman scattering investigation – art. no. 144202. Physical Review B 6314, 4202, NIL.4169-NIL.4175.
Hedoux, A., Guinet, Y., Descamps, M., 2001b. Size dependence of the Raman spectra in an amorphous-nanocrystalline mixed phase: the glacial state of triphenyl phosphite. Journal of Raman Spectroscopy 32, 677–688.
Hedoux, A., Ionov, R., Willart, J.F., Lerbret, A., Affouard, F., Guinet, Y., Descamps, M., Prevost, D., Paccou, L., Danede, F., 2006. Evidence of a two-stage thermal denaturation process in lysozyme: a Raman scattering and differ-

ential scanning calorimetry investigation. Journal of chemical physics 124, 14703.
Hedoux, A., Guinet, Y., Capet, F., Paccou, L., Descamps, M., 2008. Evidence for a high-density amorphous form in indomethacin from Raman scattering investigations. Physical Review B Condensed Matter and Materials Physics 77, 094205-094201-094210.
Hédoux, A., Guinet, Y., Descamps, M., Bénabou, A., 2000. Raman scattering investigations of the glaciation process in triphenylphosphite. Journal of Physical Chemistry B 104, 11774–11780.
Hédoux, A., Guinet, Y., Derollez, P., Hernandez, O., Paccou, L., Descamps, M., 2006. Microstructural investigations in the glacial state of triphenyl phosphite. Journal of Non-Crystalline Solids 352, 4994–5000.
Hédoux, A., Paccou, L., Guinet, Y., Willart, J.-F., Descamps, M., 2009. Using the low-frequency Raman spectroscopy to analyze the crystallization of amorphous indomethacin. European Journal of Pharmaceutical Sciences 38, 156–164.
Hernandez, O., Hédoux, A., Lefebvre, J., Guinet, Y., Descamps, M., Papoular, R., Masson, O., 2002. Ab initio structure determination of triphenyl phosphite by powder synchrotron X-ray diffraction. Journal of Applied Crystallography 35, 212–219.
Jou, H.-J., Lusk, M.T., 1997. Comparison of Johnson–Mehl–Avrami–Kologoromov kinetics with a phase-field model for microstructural evolution driven by substructure energy. Physical Review B Condensed Matter 55, 8114–8121.
Kaneniwa, N., Otsuka, M., Hayashi, T., 1985. Physicochemical characterization of indomethacin polymorphs and the transformation kinetics in ethanol. Chemical and Pharmaceutical Bulletin 33, 3447–3455.
Kistenmacher, T.J., Marsh, R.E., 1972. Crystal and molecular structure of an antiinflammatory agent, indomethacin, 1-(p-chlorobenzoyl)-5-methoxy-2-methylindole-3-acetic acid. Journal of the American Chemical Society 94, 1340–1345.
Kogermann, K, Aaltonen, J., Strachan, C.J., Pollanen, K., Veski, P., Heinamaki, J., Yliruusi, J., Rantanen, J., 2007. Qualitative in situ analysis of multiple solide-state forms using spectroscopy and partial least squares discriminant modeling. Journal of Pharmaceutical Sciences 96, 1802–1820.
Lehmann, C., Stowasser, F., 2007. The crystal structure of anhydrous beta-caffeine as determined from X-ray powder-diffraction data. Chemistry European Journal 13, 2908–2911.
Lehto, V.P., Laine, E., 1998. A kinetic study of polymorphic transition of anhydrous caffeine with micocalorimeter. Thermocimica Acta 317, 47–58.
Long, D.A., 1977. Raman Spectroscopy. McGraw-Hill International Book Company.
Malinovski, V.K., Novikov, V.N., Sokolov, A.P., 1991. Log-normal spectrum of low-energy vibrational excitations in glasses. Physics Letters A 153, 63–66.
Matsumoto, T., Zografi, G., 1999. Physical properties of solid molecular dispersions of indomethacin with poly(vinylpyrrolidone) and poly(vinylpyrrolidone-co-vinylacetate) in relation to indomethacin crystallization. Pharmaceutical research 16, 1722–1728.
McDonald, T.R.R., Beevers, C.A., 1952. The crystal and Molecular structure of alpha-glucose. Acta Crystallographica 5, 654–659.
Mishima, O., Calvert, L.D., Whalley, E., 1984. 'Melting ice' I at 77 K and 10 kbar: a new method of making amorphous solids. Nature 310, 393–395.
Mishima, O., Calvert, L.D., Whalley, E., 1985. An apparently first-order transition between two amorphous phases of ice induced by pressure. Nature 314, 76–78.
Novikov, V.N., Duval, E., 1994. A model of low-frequency Raman scattering in glasses: comparison of Brillouin and Raman data. Journal of Chemical Physics 102, 4691–4698.
Okumura, T., Otsuka, M., 2005. Evaluation of the microcrystallinity of a drug substance, indomethacin, in a pharmaceutical model tablet by chemometric FT-Raman spectroscopy. Pharmaceutical research 22, 1350–1357.
Otsuka, M., Kaneniwa, N., 1988. A kinetic study of the crystallization process of noncrystalline indomethacin under isothermal conditions. Chemical and Pharmaceutical Bulletin 36, 4026–4032.
Otsuka, M., Matsumoto, T., Kaneniwa, N., 1986. Effect of environmental temperature on polymorphic solid-state transformation of indomethacin during grinding. Chemical and Pharmaceutical Bulletin 34, 1784–1793.
Pelous, J., Levelut, C., Foret, M., Vacher, R., 1995. Low-frequency Raman scattering in oxide glasses. Philosophical Magazine 71, 693–700.
Price, C.W., 1990. Use of Kolmogorov–Johnson–Mehl–Avrami kinetics in recrystallization of metals and crystallization of metallic glasses. Acta Metallurgica et Materialia 38, 727–738.
Rolland, J.-P., Sauvajol, J.-L., 1986. Raman studies of orientationl glassy phase: the 1-cyanoadamantane glassy crystal phase. Journal of Physics C 19, 3475–3486.
Schmidt, A.G., Wartewig, S., Picker, K.M., 2004. Polyethylene oxides: protection potential against polymorphic transitions of drugs? Journal of Raman Spectroscopy 35, 360–367.
Senker, J., Rossler, E., 2001. Triphenyl phosphite: a candidate for liquid polyamorphism. Chemical Geology 174, 143–156.
Shakhtshneider, T.P., Danede, F., Capet, F., Willart, J.-F., Descamps, M., Paccou, L., Surov, E.V., Boldyreva, E.V., Boldyrev, V.V., 2007. Grinding of drugs with pharmaceutical excipients at cryogenic temperatures Part II. Cryogenic grinding of indomethacin-polyvinylpyrrolidone mixtures. Journal of Thermal Analysis and Calorimetry 89, 709–715.
Shuker, R., Gammon, R., 1970. Raman-scattering selection-rule breaking and the density of states in amorphous materials. Physical Review Letters 25, 222–225.
Strachan, C.J., Pratiwi, D., Gordon, K.C., Rades, T., 2004. Quantitative analysis of polymorphic mixtures of carbamazepine by Raman spectroscopy and principal components analysis. Journal of Raman Spectroscopy 35, 347–352.
Tanaka, H., Kurita, R., Mataki, H., 2004. Liquid-liquid transition in the molecular liquid triphenyl phosphite. Physical Review Letters 92, 025701/025701-025704.
Taylor, L.S., Zografi, G., 1997. Spectroscopic characterization of interactions between PVP and indomethacin in amorphous molecular dispersions. Pharmaceutical Research 14, 1691–1698.
Taylor, L.S., Zografi, G., 1998. The quantitative analysis of crystallinity using FT-Raman spectroscopy. Pharmaceutical Research 15, 755–761.
Vankeirsbilck, T., Vercauteren, A., Baeyens, W., Van der Weken, G., Verpoort, F., Vergote, G., Remon, J., 2002. Applications of Raman spectroscopy in pharmaceutical analysis. Trends in Analytical Chemistry 21, 869–877.
Watanabe, T., Wakiyama, N., Usui, F., Ikeda, M., Isobe, T., Senna, M., 2001. Stability of amorphous indomethacin compounded with silica. International Journal of Pharmaceutics 226, 81–91.
Wilding, M.C., Wilson, M., McMillan, P.F., 2006. Structural studies and polymorphism in amorphous solids and liquids at high pressure. Chemical Society Reviews 35, 964–986.
Willart, J.-F., Descamps, M., 2008. Solid state amorphization of pharmaceuticals. Molecular Pharmaceutics 5, 905–920.
Williams, R., Dunjer, K., 1981. Determination of the secondary structure of proteins from the amide I band of the laser spectrum. Journal of Molecular Biology 152, 783–813.
Wu, T., Yu, L., 2006a. Origin of enhanced crystal growth kinetics near T_g probed with indomethacin polymorphs. Journal of Physical Chemistry Part B: Condensed Matter, Materials, Surfaces, Interfaces and Biophysical 110, 15694–15699.
Wu, T., Yu, L., 2006b. Surface crystallization of indomethacin below T(g). Pharmaceutical Research 23, 2350–2355.
Wypych, A., Guinet, Y., Hédoux, A., 2007. Isothermal transformation of supercooled liquid n-butanol near the glass transition: polyamorphic transitions in molecular liquids investigated using Raman scattering. Physical Review B76, 144202.
Yamamoto, K., Nakano, M., Arita, T., Takayama, Y., Nakai, Y., 1970. Dissolution behavior and bioavailability of phenytoin from a ground mixture with microcrystalline cellulose. Journal of Pharmaceutical Sciences 65, 1484–1488.
Yang, Q.W., Flament, M.P., Siepmann, F., Busignies, V., Leclerc, B., Herry, C., Tchoreloff, P., Siepmann, J., 2010. Curing of aqueous polymeric film cotings: importance of the coating level and type of plasticizer. European Journal of Pharmaceutics and Biopharmaceutics 74, 362–370.
Yoshioka, M., Hancock, B.C., Zografi, G., 1994. Crystallization of indomethacin from the amorphous state below and above its glass transition temperature. Journal of Pharmaceutical Sciences 83, 1700–1705.